



Decays of 1^{-+} Charmoniumlike Hybrid

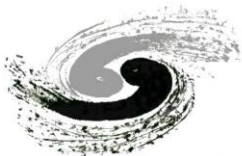
Chunjiang Shi

IHEP, CAS

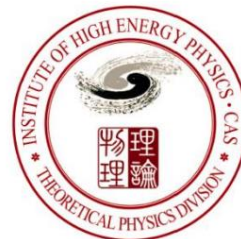
Collaborate with Ying Chen, Ming Gong, Xiangyu Jiang, Zhaofeng Liu, Wei Sun.

March 1st, 2024, **QWG 24** @ IISER Mohali, India

Based on: [arXiv:hep-lat/2306.12884](https://arxiv.org/abs/2306.12884)



中国科学院高能物理研究所
Institute of High Energy Physics
Chinese Academy of Sciences



中国科学院大学
University of Chinese Academy of Sciences

Outline

- Motivation
- Lattice methodology
- Lattice results
- Experimental prediction
- Summary

Introduction

➤ 1. Exotic hadrons:

- tetraquark / pentaquark states and hadronic molecule.
- Glueball
- hybrids ($q\bar{q}g$).

➤ 2. Experimental candidates for hybrids

➤ Isovector 1^{-+} states:

- $\pi_1(1400) / \pi_1(1600)$, $\Gamma_{tot} \sim 240\text{MeV}$
- $\pi_1(2105)$

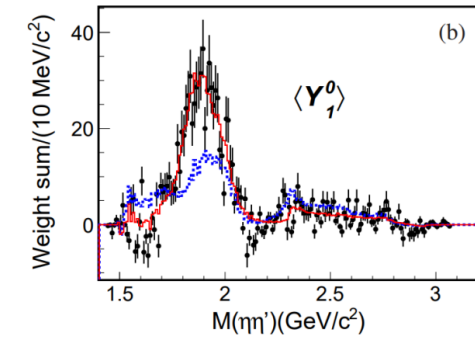
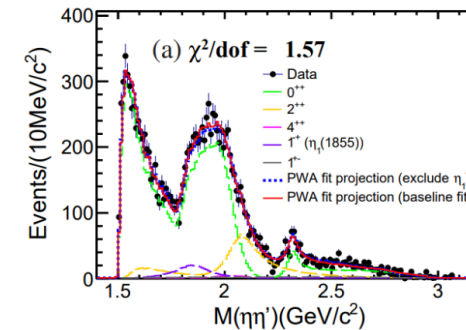
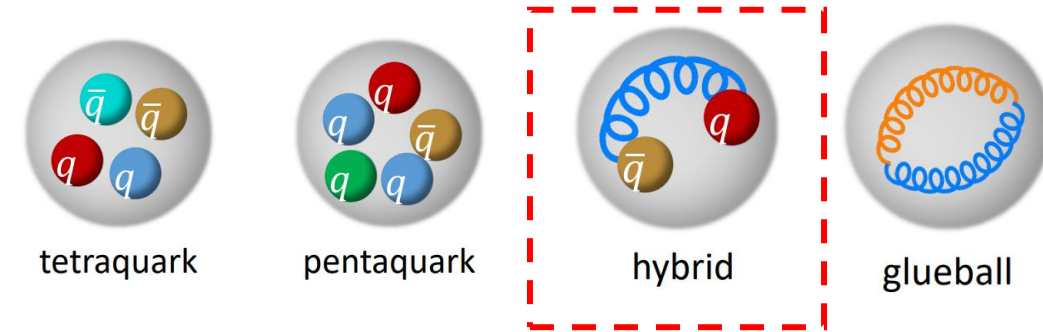
➤ Isoscalar 1^{-+} states: $\eta_1(1855)$.

➤ charmoniumlike 1^{-+} counterpart $\eta_{c1}(c\bar{c}g)$ of $\eta_1(1855)$. Exists?

➤ 3. Insights of the masses of hybrids predicted by Lattice QCD

➤ $m_{\pi_1} \sim 1.8 - 2.0 \text{ GeV}, \quad m_{\eta_1} \sim 2.0 - 2.3 \text{ GeV},$

➤ $m_{\eta_{c1}} \sim 4.2 - 4.4 \text{ GeV}.$



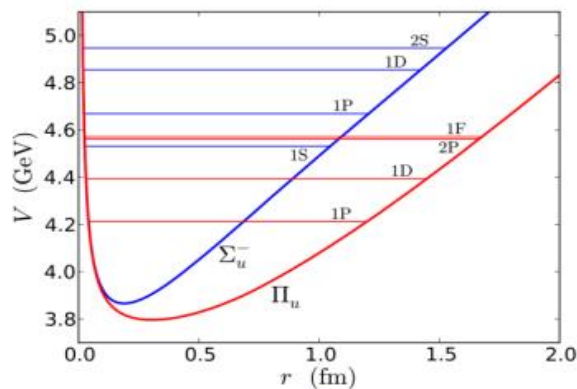
$\eta_1(1855)$ from $J/\psi \rightarrow \gamma \eta_1 \rightarrow \gamma \eta \eta'$

[BESIII : PRD.107,079901 \(2023\)](#)

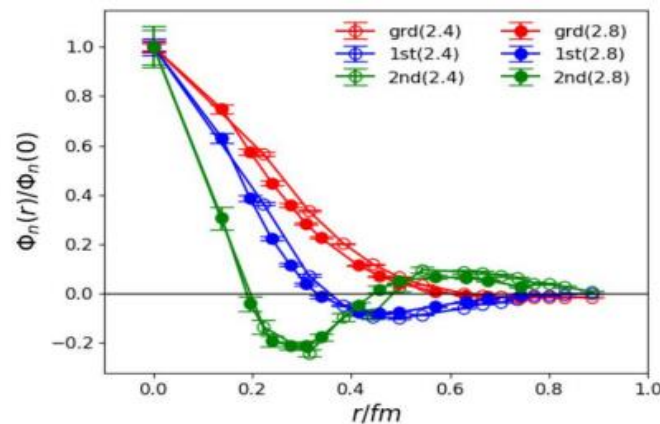
[BESIII : PRL.130,159901 \(2023\)](#)

Spectrum of charmoniumlike 1^{-+}

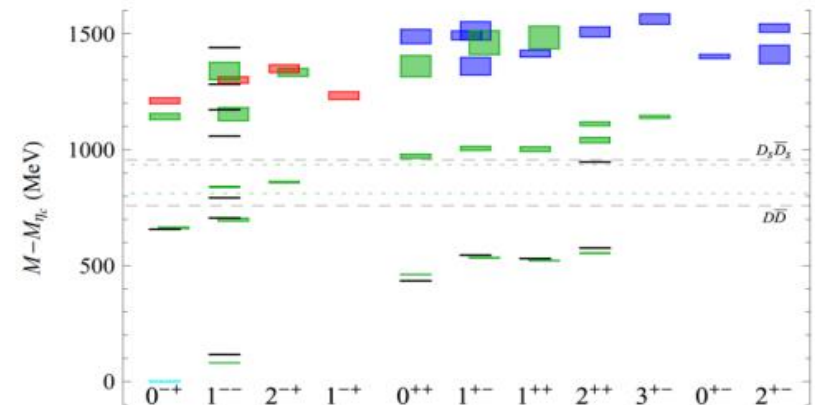
- Super-multiplet $((0, 1, 2)^{-+}, 1^{--})$ observed around 4.2 GeV
- Consistent with the phenomenological expectation.
- Non-consistence appears in the spectrum of excited states
 Flux-tube: $\Delta m(2P - 1P) \sim 0.38 \text{ GeV}$
 QLQCD: $\Delta m(2P - 1P) \sim 1.2 - 1.3 \text{ GeV}$
- The internal structure of these hybrids reflected by the BS wave functions seems different from the flux-tube picture.



E. Braaten et al.,
 Phys. Rev. D 90 (2014) 014044



Y. Ma et al., Chin. Phys. C 45 (2021) 093111



$$m_{\eta_{c1}} \approx 4.23 \text{ GeV} \quad (N_f = 2 + 1)$$

L. Liu [HSC Collab.], JHEP 07 (2012) 126

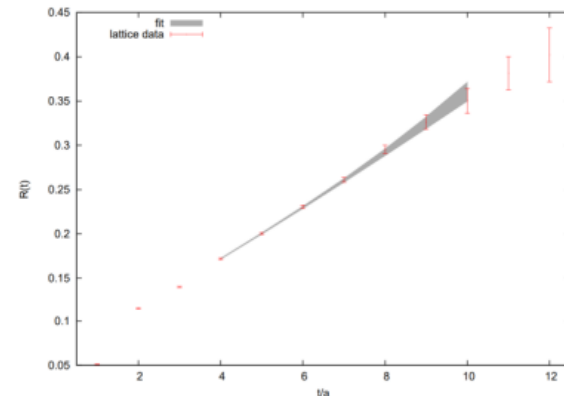
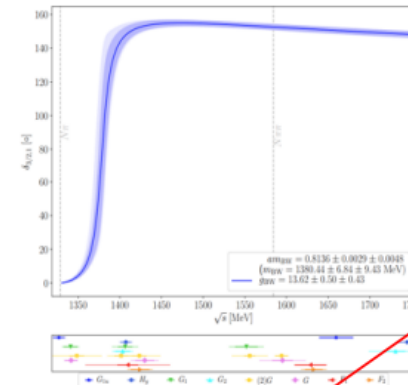
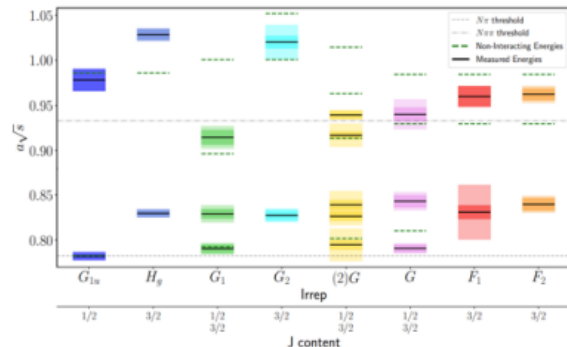
#node	$m(1^{--})$ (GeV)	$m(0^{-+})$ (GeV)	$m(1^{-+})$ (GeV)	$m(2^{-+})$ (GeV)
0	3.109(5)	3.010(4)	-	-
0	3.703(82)	3.672(76)	-	-
0	4.591(69)	4.551(63)	4.309(2)	4.419(3)
1	5.460(31)	5.393(28)	5.693(12)	5.779(12)
2	8.226(99)	8.286(109)	7.661(31)	7.708(29)

Lattice methodology: M&M method [\(C. McNeile & C. Michael, PLB 556 \(2003\) 177\)](#)

$N\pi$ scattering and the Δ resonance

G. Silvi et al., PRD103 (2021) 094508 (arXiv:2101.00689) and references therein

$N_s^3 \times N_t$	$24^3 \times 48$
β	3.31
$am_{u,d}$	-0.09530
am_s	-0.040
a [fm]	0.1163(4)
L [fm]	2.791(9)
m_π [MeV]	255.4(1.6)
$m_\pi L$	3.61(2)
N_{config}	600
N_{meas}	9600



C. Alexandrou et al.,
Phys. Rev. D 88 (2013) 031501

K -matrix rescaled: $K = \rho^{1/2} \hat{K} \rho^{1/2}$

K relates to the phase shift: $K^{Jl} = \tan \delta_{Jl}$

Breit Wigner: $\hat{K}^{(3/2,1)} = \frac{\sqrt{s}\Gamma(s)}{(m_{BW}^2 - s)\rho}$

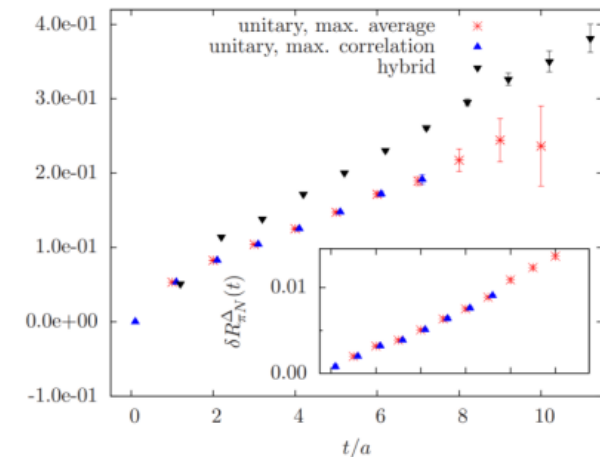
$$\Gamma(s) = \frac{g_{BW}^2 k^3}{6\pi s}$$

$$m_\Delta = (1378.3 \pm 6.6 \pm 9.0) \text{ MeV}$$

$$\Gamma_\Delta = (16.4 \pm 1.0 \pm 1.4) \text{ MeV}$$

$$\Gamma_{\text{EFT}}^{\text{LO}} = \frac{g_{\Delta-\pi N}^2 E_N + m_N}{48\pi} \frac{k^3}{E_N + E_\pi m_N^2}$$

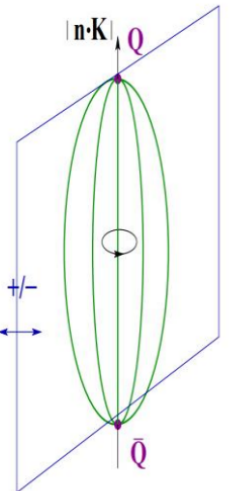
Collaboration	m_π [MeV]	Methodology	m_Δ [MeV]	$g_{\Delta-\pi N}$
Verduci 2014 [38]	266(3)	Distillation, Lüscher	1396(19) _{BW}	19.90(83)
Alexandrou et al. 2013 [37]	360	Michael, McNeile	1535(25)	27.0(0.6)(1.5)
Alexandrou et al. 2016 [39]	180	Michael, McNeile	1350(50)	23.7(0.7)(1.1)
Andersen et al. 2018 [41]	280	Stoch. distillation, Lüscher	1344(20) _{BW}	37.1(9.2)
Our result	255.4(1.6)	Smearred sources, Lüscher	1380(7)(9) _{BW} , 1378(7)(9) _{pole}	23.8(2.7)(0.9)
Physical value [5]	139.5704(2)	phenomenology, K-matrix	1232(1) _{BW} , 1210(1) _{pole}	29.4(3) [79], 28.6(3) [80]



C. Alexandrou et al.,
Phys. Rev. D 93 (2016) 114515

Flux tube model

- A vibrational string along the $Q\bar{Q}$ axis.
- The picture is originated from the lattice QCD formulation.



In analogy with **di-atomic molecule**:

Λ_η^ξ —cylinder symmetry along the $Q\bar{Q}$ axis

$|\vec{n} \cdot \mathbf{K}| = 0, 1, 2, \dots \Rightarrow \Lambda = \Sigma, \Pi, \Delta, \dots$

η : CP of the flux tube, $CP = +, - (g, u)$

ϵ : reflection symmetry with respect to the plane including the $Q\bar{Q}$ axis

Spin of the meson : $J = L + S$

$L = L_{Q\bar{Q}} + K$

$L_{Q\bar{Q}}^2 = L^2 - 2\Lambda^2 + K^2 + \dots$

PC of the meson :

$P = \epsilon(-1)^{L+\Lambda+1}, C = \eta\epsilon(-1)^{L+\Lambda+S}$

Figure 1: Quarkonium hybrid symmetries.

K. Juge et al., Phys. Rev. Lett. 82, 4400 (1999)

$$H = -\frac{1}{2\mu} \frac{\partial^2}{\partial r^2} + \frac{L(L+1) - \Lambda^2}{2\mu r^2} + E^1(r)$$

$$E^1(r) = -\frac{4\alpha_s}{3r} + c + br + \frac{\pi}{r} (1 - e^{-fb^{1/2}r})$$

TABLE I. Some low-lying meson hybrids.

Flavor	J^{PC} or J^P	Mass (GeV) for $f=1$	$\frac{dm}{df}$ (GeV)	Δm^a (GeV)	m^b (GeV)
$I=1$	$2^{\pm\mp}, 1^{\pm\mp}, 0^{\pm\mp}, 1^{\pm\pm}$	1.67	0.08	0.19	~ 1.9
$I=\frac{1}{2}$	$2^\pm, 1^\pm, 0^\pm, 1^\pm$	1.80	0.10	0.17	~ 2.0
$I=0$ $\left[\frac{u\bar{u} + d\bar{d}}{\sqrt{2}} \right]$	$2^{\pm\mp}, 1^{\pm\mp}, 0^{\pm\mp}, 1^{\pm\pm}$	1.67	0.08	0.19	~ 1.9
$I=0$ ($s\bar{s}$)	$2^{\pm\mp}, 1^{\pm\mp}, 0^{\pm\mp}, 1^{\pm\pm}$	1.91	0.12	0.14	~ 2.1
$c\bar{c}$	$2^{\pm\mp}, 1^{\pm\mp}, 0^{\pm\mp}, 1^{\pm\pm}$	4.19	0.18	0.06	~ 4.3
$b\bar{b}$	$2^{\pm\mp}, 1^{\pm\mp}, 0^{\pm\mp}, 1^{\pm\pm}$	10.79	0.28	0.02	~ 10.8

^aContribution to the mass from nonadiabatic effects, taken from Ref. 14.

^bA “best guess” based on the previous columns.

Isgur & Paton, Phys. Rev. D 31 (1985) 2910

Hybrid in the Flux tube model

Flux-tube model has selection rule:

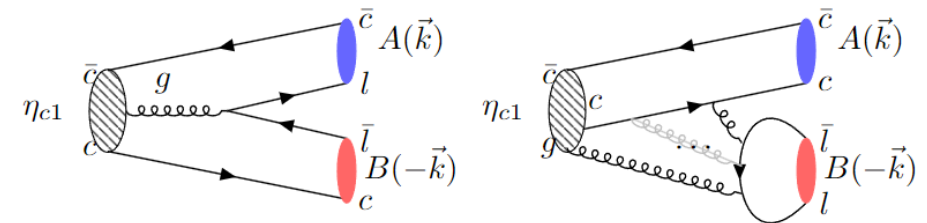
(P. Page et al., Phys.Rev.D 59 (1999) 034016)

$$\langle AB|H_I|H\rangle \propto \int d^3\vec{r}(\phi_H(\vec{r}) \dots) \int_0^1 d\xi \cos(\xi\pi) \cdot \phi_A(\xi\vec{r}) \cdot \phi_B((1-\xi)\vec{r})$$

- 1) Modes of two S-wave mesons are **suppressed**, SP-modes are **favored**.
- 2) Modes of two identical mesons are **prohibited**.

Open-charm and closed-charm decay modes

- 1) SP modes : $D_1\bar{D}, \chi_{c1}\eta(\eta')$
- 2) SS modes : $D^*\bar{D}, D^*\bar{D}^*, \eta_c\eta(\eta'), J/\psi\omega(\phi)$



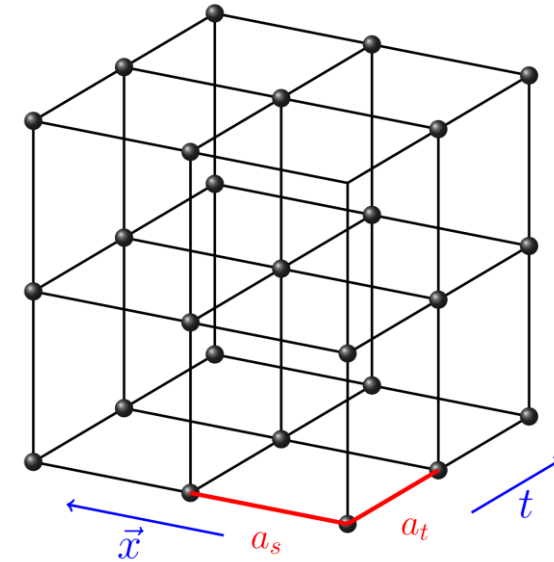
Lattice setup

- Tadpole improved Symanzik's gauge action
(C. Morningstar, PRD60(1999)034509)
- **Anisotropic** Lattice
- $N_f = 2$ **clover** gauge ensembles with degenerate u, d quarks

IE	$N_s^3 \times N_t$	β	$a_t^{-1}(\text{GeV})$	ξ	$m_\pi(\text{MeV})$	N_V	N_{cfg}
L16	$16^3 \times 128$	2.0	6.894(51)	~ 5.3	~ 350	70	708
L24	$24^3 \times 192$	2.0	6.894(51)	~ 5.3	~ 350	160	171

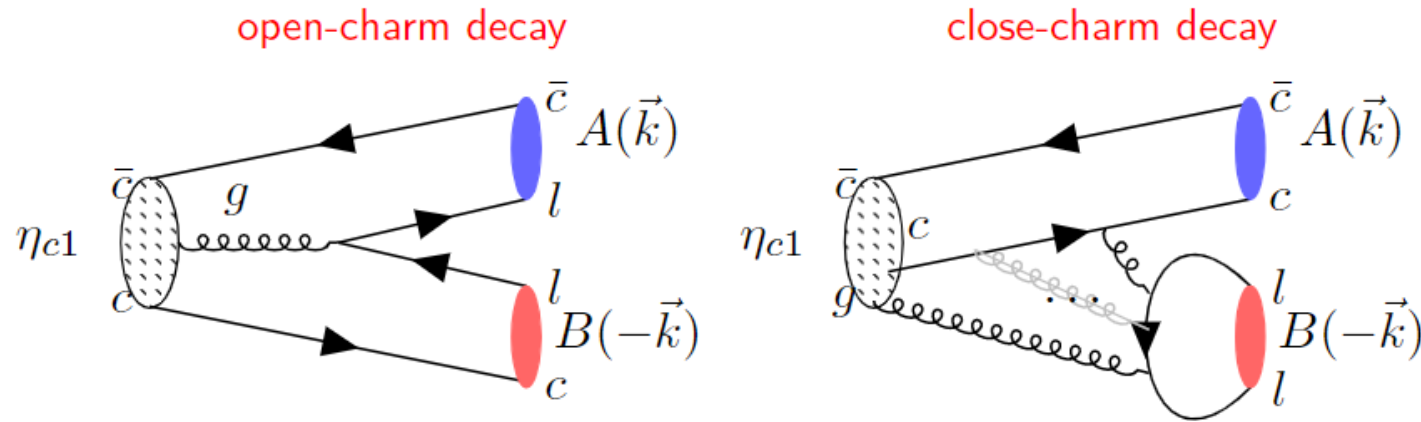
See: Jiang et al, Phys.Rev.D 107 (2023) 094510

- **Distillation method**:
(M.Peardon et al.(HSC.)(2009)PRD80,054506)
- **disconnected** diagrams are involved



$$a_s/a_t = 5.3$$

η_{c1} decay modes



open-charm decay: $D\bar{D}_1$ (S -wave), $D\bar{D}^*$ (P -wave), $D^*\bar{D}^*$ (P -wave).
 close-charm decay: $\chi_{c1}\eta$ (S -wave), $\eta_c\eta'$ (P -wave), $J/\psi\omega$ (P -wave).

- The flavor wave functions of the open-charm modes

$$|D\bar{D}'\rangle_{(C=+)}^{(I=0)} = \frac{1}{2}(|D^+D'^-\rangle + |D^0\bar{D}'^0\rangle) \pm \frac{1}{2}(|D^-D'^+\rangle + |\bar{D}^0D'^0\rangle)$$

$D' = D^*, D_1,$
 "+" for $D\bar{D}^*$
 "-" for $D\bar{D}_1$

$$|D^*\bar{D}^*\rangle_{(C=+)}^{(I=0)} = \frac{1}{\sqrt{2}}(|D^{*+}D^{*-}\rangle + |D^{*0}\bar{D}^{*0}\rangle)_{(L=1)}^{(S=1)}$$

$L + S = \text{even}$

Decay amplitudes in M&M method

Effective Lagrangian:

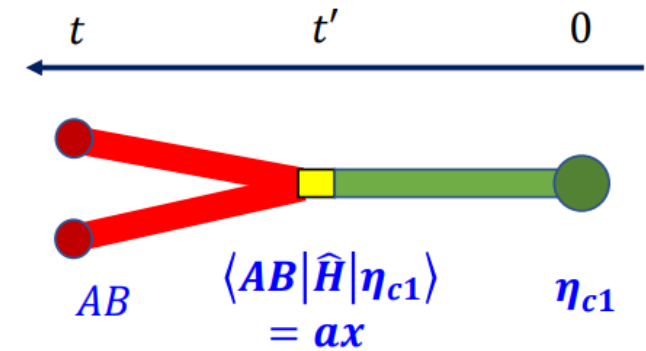
$$\mathcal{L}_I^{\text{cc}} \sim -g_{\chi\eta} m_{\eta_{c1}} H_\mu A^\mu \eta - ig_{\eta_c\eta} H_\mu \eta_c \overleftrightarrow{\partial}^\mu \eta + iH_\mu \left(g\psi_\nu \partial^\nu \omega^\mu + g'\omega_\nu \partial^\nu \psi^\mu + g_0\psi_\nu \overleftrightarrow{\partial}^\mu \omega^\nu \right),$$

$$\begin{aligned} \mathcal{L}_I^{\text{oc}} \sim & g_{D_1 D} m_{\eta_{c1}} H_\mu \frac{1}{2} \left(D_1^{\mu,\dagger} D + D^\dagger D_1^\mu \right) \\ & + g_{D^* \bar{D}^*} H^\mu \frac{i}{\sqrt{2}} \left(D^{\nu,\dagger} \partial_\nu D_\mu + \partial_\nu D_\mu^\dagger D^\nu \right) \\ & + \frac{g_{D^* \bar{D}^*}}{m_{\eta_{c1}}} \epsilon^{\mu\nu\rho\sigma} (\partial_\mu H_\nu) \frac{1}{2} \left[(\partial_\rho D_\sigma^\dagger) D - D^\dagger (\partial_\rho D_\sigma) \right]. \end{aligned}$$

$$\begin{aligned} |\eta_{c1}\rangle &= \begin{pmatrix} 1 \\ 0 \end{pmatrix} & |AB\rangle &= \begin{pmatrix} 0 \\ 1 \end{pmatrix} \\ \hat{H} &= \begin{pmatrix} m_{\eta_{c1}} & x \\ x & E_{AB} \end{pmatrix} & \longrightarrow & \hat{T}(a) = e^{-a\hat{H}} = e^{-a\bar{E}} \begin{pmatrix} e^{-a\Delta/2} & ax \\ ax & e^{a\Delta/2} \end{pmatrix} \\ & & & \bar{E} = \frac{m_{\eta_{c1}} + E_{AB}}{2}, \quad \Delta = m_{\eta_{c1}} - E_{AB} \end{aligned}$$

$$\begin{aligned} x_{AP}^{\lambda'\lambda} &= g_{AP} m_{\eta_{c1}} \vec{\epsilon}_\lambda(\vec{0}) \cdot \vec{\epsilon}_{\lambda'}^*(\vec{k}), \\ x_{PP}^\lambda &= 2g_{PP} \vec{\epsilon}_\lambda(\vec{0}) \cdot \vec{k}, \\ x_{VP}^{\lambda'\lambda} &= g_{VP} \vec{\epsilon}_\lambda(\vec{0}) \cdot (\vec{\epsilon}_{\lambda'}^*(\vec{k}) \times \vec{k}), \\ x_{D^* \bar{D}^*}^{\lambda'\lambda''\lambda} &= 2g_{D^* \bar{D}^*} \vec{\epsilon}_\lambda(\vec{0}) \cdot \left(\vec{k} \times \left[\vec{\epsilon}_{\lambda'}^*(\vec{k}) \times \vec{\epsilon}_{\lambda''}^*(-\vec{k}) \right] \right), \end{aligned}$$

$$\langle \Omega | \mathcal{O}_{AB} | \eta_{c1} \rangle \approx 0 \quad \langle \Omega | \mathcal{O}_{\eta_{c1}} | AB \rangle \approx 0$$



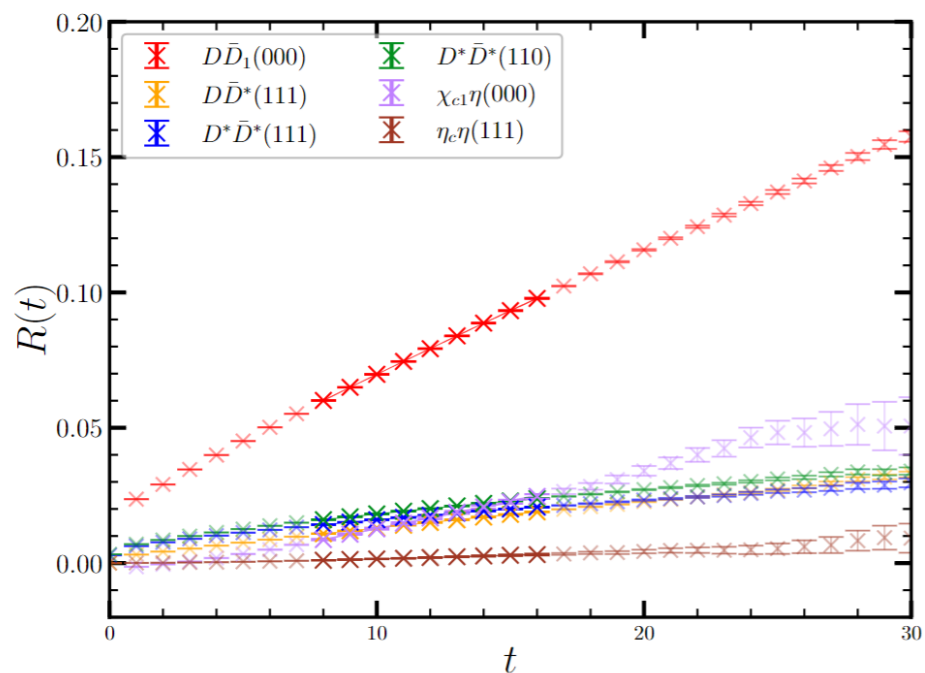
Lattice results

$$\begin{aligned}
 \mathcal{C}_{\eta_{c1}, AB}(t) &= \langle \Omega | \mathcal{O}_{AB}(t) \mathcal{O}_{\eta_{c1}}^+(0) | \Omega \rangle \\
 &= \langle \Omega | \mathcal{O}_{AB}(0) e^{-t a \hat{H}} \mathcal{O}_{\eta_{c1}}^+(0) | \Omega \rangle \\
 &\rightarrow -axt e^{-t a \bar{E}} \langle \Omega | \mathcal{O}_{AB} | AB \rangle \langle \eta_{c1} | \mathcal{O}_{\eta_{c1}}^+ | \Omega \rangle
 \end{aligned}$$

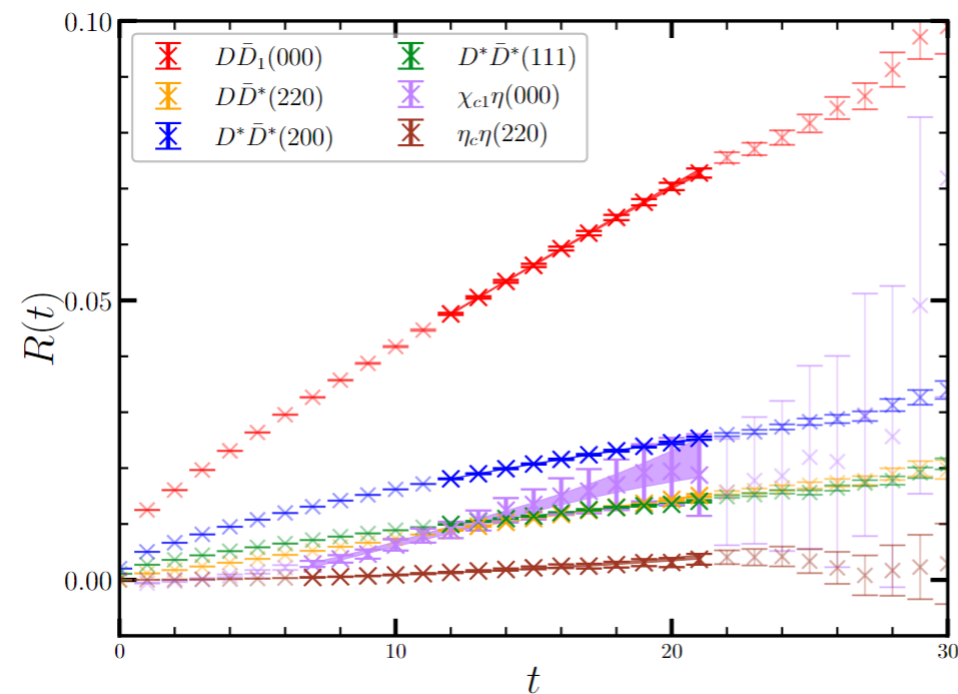


transition
amplitude

$$\frac{\mathcal{C}_{\eta_{c1}, AB}(t)}{\sqrt{\mathcal{C}_{\eta_{c1}}(t) \mathcal{C}_A(t) \mathcal{C}_B(t)}} \rightarrow -(ax) t \left(1 + \frac{1}{24} (a\Delta t)^2 \right)$$



L16



L24

Numerical results

Mode (AB)	\hat{k} (IE)	r_1 ($\times 10^{-3}$)	g_{AB}	g_{AB} (ave.)	Γ_{AB} (MeV)
$D_1 \bar{D}$	(0, 0, 0)(L16)	4.95(5)	4.27(5)	4.6(6)	258(133)
	(0, 0, 0)(L24)	3.10(26)	4.92(41)		
$D^* \bar{D}$	(1, 1, 1)(L16)	1.11(3)	8.35(21)	8.3(7)	88(18)
	(2, 2, 0)(L24)	0.78(7)	8.34(74)		
$D^* \bar{D}^*$	(1, 1, 1)(L16)	1.00(3)	3.44(12)	4.6(1.8)	150(118)
	(1, 1, 0)(L16)	1.15(4)	3.79(12)		
	(2, 0, 0)(L24)	1.05(9)	5.06(42)		
	(1, 1, 1)(L24)	0.67(7)	6.31(58)		
$\chi_{c1} \eta_{(2)}$	(0, 0, 0)(L16)	2.04(26)	1.31(2)	1.35(45)	-
	(0, 0, 0)(L24)	1.18(38)	1.39(45)		
$\eta_c \eta_{(2)}$	(1, 1, 1)(L16)	0.20(6)	0.62(18)	0.55(22)	-
	(2, 2, 0)(L24)	0.10(3)	0.47(12)		

$$|\overline{\mathcal{M}(\eta_{c1} \rightarrow AP)}|^2 = \frac{1}{3} g_{AP}^2 m_{\eta_{c1}} \left(3 + \frac{k_{\text{ex}}^2}{m_A^2} \right),$$

$$|\overline{\mathcal{M}(\eta_{c1} \rightarrow PP)}|^2 = \frac{4}{3} g_{PP}^2 k_{\text{ex}}^2,$$

$$|\overline{\mathcal{M}(\eta_{c1} \rightarrow VP)}|^2 = \frac{2}{3} g_{VP}^2 k_{\text{ex}}^2,$$

$$|\overline{\mathcal{M}(\eta_{c1} \rightarrow D^* \bar{D}^*)}|^2 = \frac{4}{3} g^2 k_{\text{ex}}^2 \frac{m_{\eta_{c1}}^2}{m_{D^*}^2}.$$

$$\Gamma_{AB} = \frac{1}{8\pi} \frac{k_{\text{ex}}}{m_{\eta_{c1}}^2} |\overline{\mathcal{M}(\eta_{c1} \rightarrow AB)}|^2$$

- $D_1 \bar{D}$ dominates.
- $D^* \bar{D}$ and $D^* \bar{D}^*$ are important.

This observation is in striking contrast to the expectation of the flux-tube model.

Numerical results

Mode (AB)	\hat{k} (IE)	r_1 ($\times 10^{-3}$)	g_{AB}	g_{AB} (ave.)	Γ_{AB} (MeV)
$D_1 \bar{D}$	(0, 0, 0)(L16)	4.95(5)	4.27(5)	4.6(6)	258(133)
	(0, 0, 0)(L24)	3.10(26)	4.92(41)		
$D^* \bar{D}$	(1, 1, 1)(L16)	1.11(3)	8.35(21)	8.3(7)	88(18)
	(2, 2, 0)(L24)	0.78(7)	8.34(74)		
$D^* \bar{D}^*$	(1, 1, 1)(L16)	1.00(3)	3.44(12)	4.6(1.8)	150(118)
	(1, 1, 0)(L16)	1.15(4)	3.79(12)		
	(2, 0, 0)(L24)	1.05(9)	5.06(42)		
	(1, 1, 1)(L24)	0.67(7)	6.31(58)		
$\chi_{c1} \eta_{(2)}$	(0, 0, 0)(L16)	2.04(26)	1.31(2)	1.35(45)	-
	(0, 0, 0)(L24)	1.18(38)	1.39(45)		
$\eta_c \eta_{(2)}$	(1, 1, 1)(L16)	0.20(6)	0.62(18)	0.55(22)	-
	(2, 2, 0)(L24)	0.10(3)	0.47(12)		

Due to $m_{\eta_{c1}} = 4.329(36)\text{GeV}$ from our lattice

$$|\overline{\mathcal{M}(\eta_{c1} \rightarrow AP)}|^2 = \frac{1}{3} g_{AP}^2 m_{\eta_{c1}} \left(3 + \frac{k_{\text{ex}}^2}{m_A^2} \right),$$

$$|\overline{\mathcal{M}(\eta_{c1} \rightarrow PP)}|^2 = \frac{4}{3} g_{PP}^2 k_{\text{ex}}^2,$$

$$|\overline{\mathcal{M}(\eta_{c1} \rightarrow VP)}|^2 = \frac{2}{3} g_{VP}^2 k_{\text{ex}}^2,$$

$$|\overline{\mathcal{M}(\eta_{c1} \rightarrow D^* \bar{D}^*)}|^2 = \frac{4}{3} g^2 k_{\text{ex}}^2 \frac{m_{\eta_{c1}}^2}{m_{D^*}^2}.$$

$$\Gamma_{AB} = \frac{1}{8\pi} \frac{k_{\text{ex}}}{m_{\eta_{c1}}^2} |\overline{\mathcal{M}(\eta_{c1} \rightarrow AB)}|^2$$

- $D_1 \bar{D}$ dominates.
- $D^* \bar{D}$ and $D^* \bar{D}^*$ are important.

This observation is in striking contrast to the expectation of the flux-tube model.

Results v.s. Flux-tube model

Mode (AB)	$\hat{k}(\text{IE})$	r_1 ($\times 10^{-3}$)	g_{AB}	g_{AB} (ave.)	Γ_{AB} (MeV)
$D_1\bar{D}$	(0, 0, 0)(L16)	4.95(5)	4.27(5)	4.6(6)	258(133)
	(0, 0, 0)(L24)	3.10(26)	4.92(41)		
$D^*\bar{D}$	(1, 1, 1)(L16)	1.11(3)	8.35(21)	8.3(7)	88(18)
	(2, 2, 0)(L24)	0.78(7)	8.34(74)		
$D^*\bar{D}^*$	(1, 1, 1)(L16)	1.00(3)	3.44(12)	4.6(1.8)	150(118)
	(1, 1, 0)(L16)	1.15(4)	3.79(12)		
	(2, 0, 0)(L24)	1.05(9)	5.06(42)		
	(1, 1, 1)(L24)	0.67(7)	6.31(58)		
$\chi_{c1}\eta_{(2)}$	(0, 0, 0)(L16)	2.04(26)	1.31(2)	1.35(45)	-
	(0, 0, 0)(L24)	1.18(38)	1.39(45)		
$\eta_c\eta_{(2)}$	(1, 1, 1)(L16)	0.20(6)	0.62(18)	0.55(22)	-
	(2, 2, 0)(L24)	0.10(3)	0.47(12)		

(Isgur& Paton 1985)

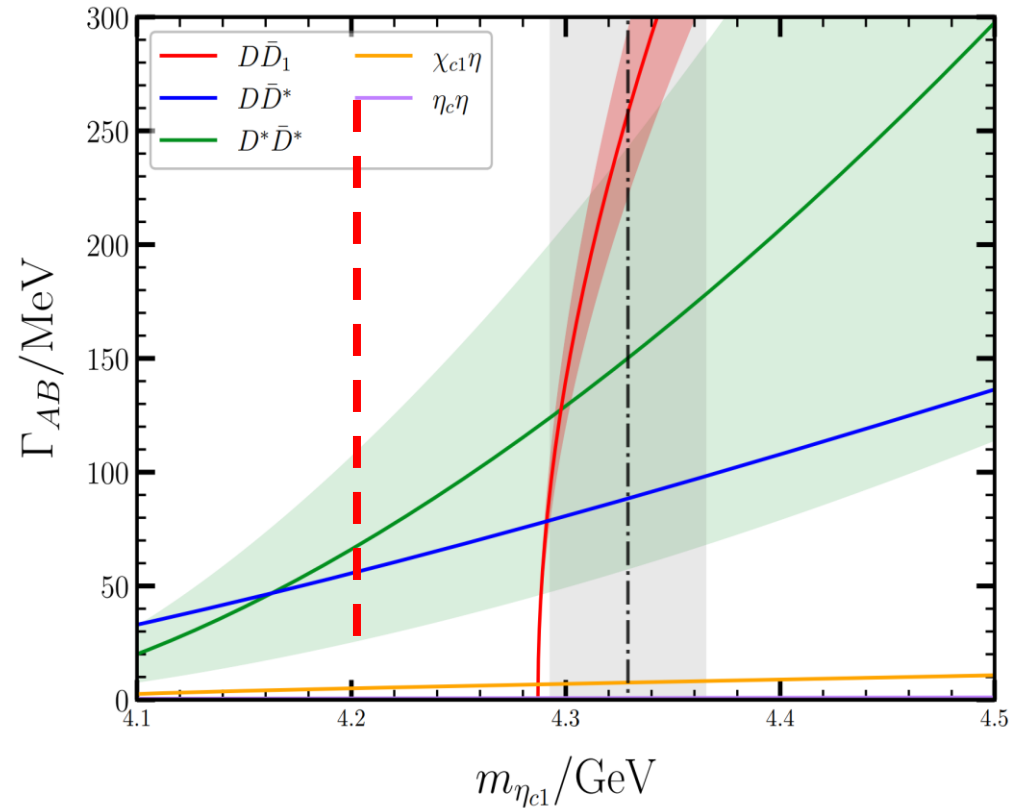
Flux tube model: light Isoscalar hybrid width $\sim 150\text{MeV}$

$c\bar{c}$ Isoscalar hybrid width $\sim 30\text{MeV}$

1^{-+}				
	D^*D	P	.5	.1
	$D^{**}(2^+)D$	D	-	.5
	$D^{**}(1_L^+)D$	S	-	1.2
		D	-	2.5
	$D^{**}(1_H^+)D$	S	-	25
		D	-	0
	Γ		.5	29

This observation is in striking contrast to the expectation of the flux-tube model.

Conclusion



- For $m_{\eta_{c1}} = 4329(36)$ MeV, we have

$$\Gamma_{D_1 \bar{D}} = 258(133) \text{ MeV}$$

$$\Gamma_{D^* \bar{D}^*} = 150(118) \text{ MeV}$$

$$\Gamma_{D \bar{D}^*} = 88(18) \text{ MeV}$$

$$\Gamma_{\chi_{c1} \eta} = \sin^2 \theta \cdot 44(29) \text{ MeV}$$

$$\Gamma_{\eta_{c1} \eta'} = \cos^2 \theta \cdot 0.93(77) \text{ MeV}$$

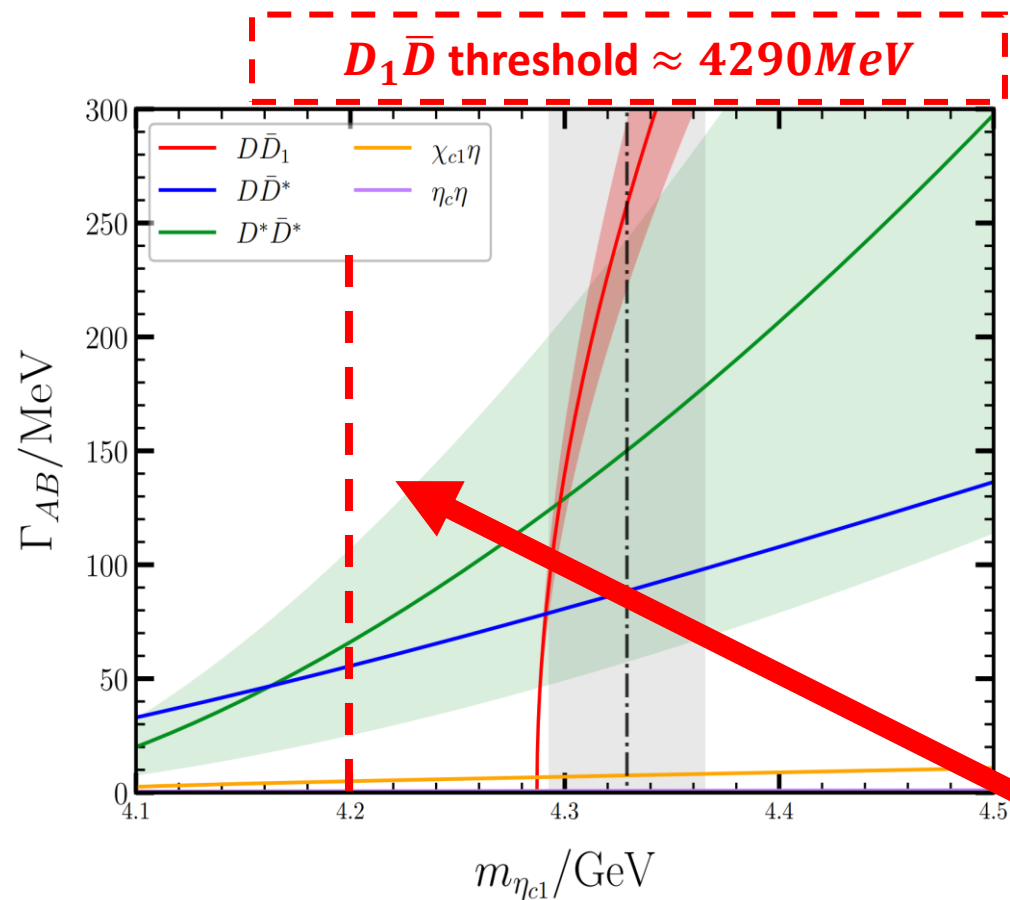
- Given the mass above, η_{c1} seems **too wide to be identified easily** in experiments.

The $m_{\eta_{c1}}$ -dependence of partial decay widths

$$|D^* \bar{D}^*\rangle_{(C=+)}^{(I=0)} = \frac{1}{\sqrt{2}} (|D^{*+} D^{*-}\rangle + |D^{0*} \bar{D}^{0*}\rangle)_{(L=1)}^{(S=1)}$$

$$L + S = \text{even}$$

- We suggest LHCb, BelleII and BESIII to search for η_{c1} in $D^* \bar{D}$ and $D^* \bar{D}^*$ systems !



The $m_{\eta_{c1}}$ -dependence of partial decay widths

$$|D^*\bar{D}^*\rangle_{(C=+)}^{(I=0)} = \frac{1}{\sqrt{2}} (|D^{*+}D^{*-}\rangle + |D^{0*}\bar{D}^{0*}\rangle)_{(L=1)}^{(S=1)}$$

$L + S = \text{even}$

- For $m_{\eta_{c1}} = 4329(36)$ MeV, we have

$$\Gamma_{D_1\bar{D}} = 258(133) \text{ MeV}$$

$$\Gamma_{D^*\bar{D}^*} = 150(118) \text{ MeV}$$

$$\Gamma_{D\bar{D}^*} = 88(18) \text{ MeV}$$

$$\Gamma_{\chi_{c1}\eta} = \sin^2 \theta \cdot 44(29) \text{ MeV}$$

$$\Gamma_{\eta_c\eta'} = \cos^2 \theta \cdot 0.93(77) \text{ MeV}$$

- Given the mass above, η_{c1} seems **too wide to be identified easily** in experiments.
- However, $\Gamma_{\eta_{c1}}$ is very sensitive to $m_{\eta_{c1}}$.**
- If $m_{\eta_{c1}} \sim 4.2$ GeV, then $\Gamma_{\eta_{c1}} \sim 100$ MeV.**
The dominant decay channels are $D^*\bar{D}$ and $D^*\bar{D}^*$.
- Especially for $D^*\bar{D}^*$, the measurement of the polarization of D^* and \bar{D}^* will help distinguish a 1^{-+} states from 1^{--} states.**

- We suggest LHCb, BelleII and BESIII to search for η_{c1} in $D^*\bar{D}$ and $D^*\bar{D}^*$ systems !

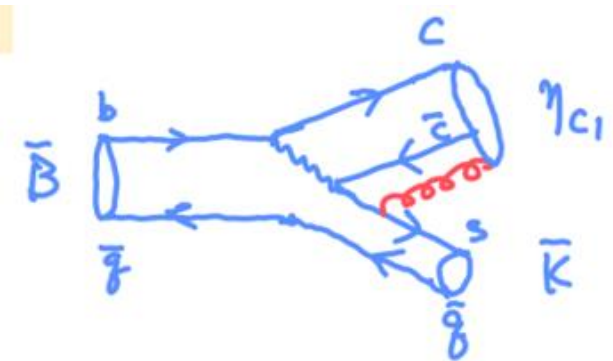
Possible production in experiments

1) η_{c1} production on e^+e^- collider experiments: (**BESIII**)

$$e^+e^- \rightarrow \psi(nS) \rightarrow \gamma\eta_{c1}$$

2) η_{c1} production from **B meson weak decay**

$$B \rightarrow \eta_{c1}\bar{K} \quad (\text{LHCb and Belle):}$$



Summary

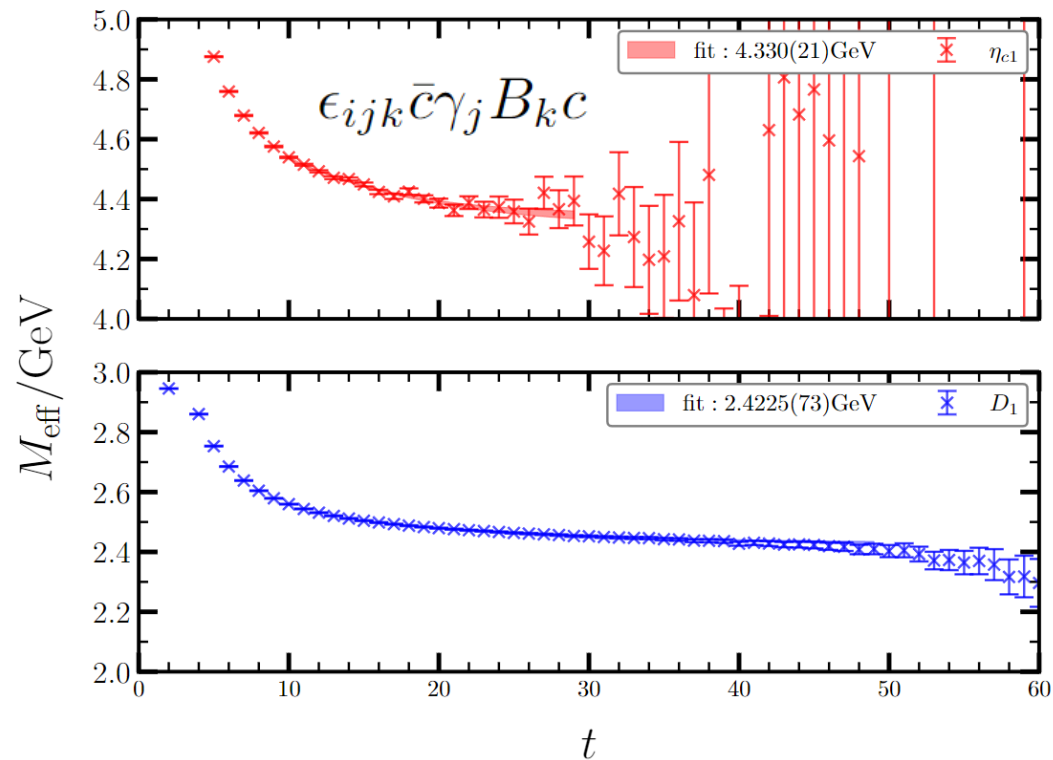
- ✓ We give **the first Lattice QCD prediction** of the **partial decay widths** of the charmoniumlike η_{c1} .
- ✓ Disfavor the results of the **Flux-tube model** (Disfavor the S-wave suppression).
- ✓ We provide the theoretical information for the **experimental search** for charmoniumlike hybrid η_{c1} .

Thank You

Backup slides

Meson spectrum on our lattice

X	ω	$\eta_{(2)}$	η_c	J/ψ	χ_{c1}	D	D^*	D_1	η_{c1}
$m_X(\text{L16})(\text{MeV})$	857(10)	715(10)	2975.0(3)	3099.1(2)	3559.8(1.7)	1882(1)	2023(1)	2423(7)	4330(21)
$m_X(\text{L24})(\text{MeV})$	845(7)	705(21)	2976.3(4)	3099.4(4)	3560.4(6.4)	1881(1)	2019(1)	2430(10)	4328(68)
$m_X(\text{PDG})(\text{MeV})$ [42]	782	547/958	2983	3097	3511	~ 1867	~ 2008	2420	-



Partial-wave operators

$$\mathcal{O}_{AB;JLSP}^M(\hat{k}) = \sum_{M_L, M_S, M_A, M_B} \langle L, M_L; S, M_S | JM \rangle \langle S_A M_A; S_B M_B | S, M_S \rangle \\ \times \sum_{R \in O_h} Y_{LM_L}^*(R \circ \vec{k}) \mathcal{O}_A^{M_A}(R \circ \vec{k}) \mathcal{O}_B^{M_B}(-R \circ \vec{k}),$$

Mode (AB)	E_{AB} (MeV)	$a_t \Delta$	r_0	$r_1 (\times 10^{-3})$	$r_3 (\times 10^{-7})$
L16	$(m_{\eta_{c1}} = 4330(21) \text{ MeV})$				
$D\bar{D}_1(000)$	4304(7)	~ 0.004	0.02077(38)	4.95(5)	-5.1(1.3)
$D\bar{D}^*(111)$	4301(4)	~ 0.004	0.00210(19)	1.11(3)	-2.2(8)
$D^*\bar{D}^*(111)$	4405(10)	~ -0.011	0.00702(25)	1.00(3)	-4.3(9)
$D^*\bar{D}^*(110)$	4288(4)	~ 0.006	0.00702(25)	1.15(4)	-4.1(9)
$\chi_{c1}\eta_{(2)}(000)$	4262(8)	~ 0.010	-0.0076(18)	2.04(26)	-0.9(6.8)
$\eta_c\eta_{(2)}(111)$	4347(39)	~ -0.003	-0.00057(39)	0.20(6)	1.6(1.6)
L24	$(m_{\eta_{c1}} = 4328(68) \text{ MeV})$				
$D\bar{D}_1(000)$	4310(10)	~ 0.003	0.0110(26)	3.10(26)	-3.3(3.5)
$D\bar{D}^*(220)$	4361(5)	~ -0.005	-0.00027(69)	0.78(7)	-1.07(97)
$D^*\bar{D}^*(200)$	4269(2)	~ 0.009	0.00598(87)	1.05(9)	-3.1(1.2)
$D^*\bar{D}^*(111)$	4216(3)	~ 0.016	0.00234(62)	0.67(7)	-2.50(83)
$\chi_{c1}\eta_{(2)}(000)$	4260(7)	~ 0.010	-0.0057(27)	1.18(38)	-3.0(9.0)
$\eta_c\eta_{(2)}(220)$	4304(25)	~ 0.004	-0.00037(17)	0.10(3)	2.49(77)

Fitting stability

